On the stability of a compressible axisymmetric rotating flow in a pipe

By Z. RUSAK AND J. H. LEE

Department of Mechanical, Aerospace, and Nuclear Engineering, Rensselaer Polytechnic Institute, Troy,
New York 12180-3590, USA

The linear stability of a compressible inviscid axisymmetric and rotating columnar flow of a prefect gas in a finite-length straight circular pipe is investigated. This work extends a previous analysis to include the influence of Mach number on the flow dynamics. A well-posed model of the unsteady motion of a swirling flow, with inlet and outlet conditions that may reflect the physical situation, is formulated. The linearized equations of motion for the evolution of infinitesimal axially symmetric disturbances are derived. A general mode of disturbance, that is not limited to the axial-Fourier mode, is introduced and an eigenvalue problem is developed. It is found that a neutral mode of disturbance exists at 'the critical swirl ratio for a compressible vortex flow'. The flow changes its stability characteristics as the swirl ratio increases across this critical level. When the swirl ratio is below the critical level (supercritical flow), an asymptotically stable mode is found and, when it is above the critical level (subcritical flow), an unstable mode of disturbance develops. This result cannot be predicted by any of the previous stability criteria. When the characteristic Mach number of the base flow tends to zero, the results are the same as found for incompressible swirling flows in pipes. The growth rate ratio is positive for all Mach numbers, but decreases as Mach number is increased. This ratio vanishes at the limit Mach number at which the critical swirl tends to infinity. The present results also demonstrate that the axisymmetric breakdown of high-Reynolds-number compressible vortex flows may be delayed to higher swirl ratios with the increase of the incoming flow Mach number.

1. Introduction

The stability of compressible swirling flows is an important problem for a variety of technological applications such as the aerodynamics of slender wings operating at high angles of incidence, combustion chambers, nozzles, and other high-speed flow devices where swirl has a dominant influence. The study of this problem may also shed light on complicated stability and breakdown phenomena that appear in numerous problems of geophysical and meteorological significance. In all of these cases, the flow Mach number is not small and may reach values of 0.2 to 0.7, and the effect of compressibility is an essential part of the flow dynamics and influences the conditions for the appearance of instabilities and transition (breakdown) phenomena.

Vortex stability and breakdown is a classical topic in fluid dynamics that was extensively studied for over 100 years. Reviews of this topic include the reports by Leibovich (1984), Escudier (1988), Delery (1994), Ash & Khorrami (1995), and Althaus, Bruecker & Weimer (1995). A variety of vortex stability criteria were

developed over the years, among them are the classical criteria of Rayleigh (1916) (later strengthened by Synge 1933), Ludwieg (1960), Howard & Gupta (1962), Lessen, Singh & Paillet (1974), and Leibovich & Stewartson (1983). These reviews show that all of the studies on this topic focused only on the incompressible flow problem. Also, they all concentrated on vortex flows in an infinite axial domain, described the disturbances by Fourier periodic modes in the axial direction, and showed that as the swirl is increased the flow becomes neutrally stable. This may lead to the conclusion that stability may not be directly related to the development of breakdown phenomena in vortex flows (Leibovich 1984). Moreover, none of the previous stability analyses investigated the effect of compressibility on the flow stability and dynamics.

Only a few numerical simulations by Melville (1996), Tromp & Beran (1996, 1997) and Herrada, Prez-Saborid & Barrero (2000) included the effect of flow Mach number on the appearance of vortex breakdown. Note that all these simulations were limited to compressible flows of perfect gases with relatively low Reynolds numbers (1000 or less) and therefore apply to only swirling flows in micro-scale pipes where viscous dissipation may dominate. Melville (1996) and Herrada *et al.* (2000) showed that increasing Mach number stabilizes the vortex flow and delays the appearance of breakdown to a higher level of swirl ratio. To the best of our knowledge, there is no computation of compressible vortex flows in pipes at realistic high Reynolds numbers (10^6 or more). Also, to the best of our knowledge, there are no detailed experimental studies of compressible vortices that may indicate the flow behaviour.

A recent set of papers by Wang & Rusak (1996*a*, *b*, 1997*a*, *b*), Rusak, Judd & Wang (1997), Rusak, Wang & Whiting (1998*a*), Rusak, Whiting & Wang (1998*b*), Rusak (1998, 2000) and Rusak & Judd (2001) studied the stability and dynamics of an incompressible and axisymmetric swirling flow in a finite-length long circular pipe. Their physical model assumed that the flow entering the pipe is generated by a vortex generator. Under a continuous and steady operation of the generator, the same profiles of the axial and circumferential velocities and of the azimuthal vorticity are imposed at all time at some cross-section downstream of the vortex generator, no matter how the flow evolves in the pipe. This cross-section is denoted as the pipe inlet. It is also assumed that the inlet state has a degree of freedom to develop a radial velocity to reflect the upstream influence by disturbances in the pipe that have the tendency to cast such an influence. At the pipe outlet a fully developed columnar state was considered. These conditions may represent the physical situations found in the experimental studies of low-speed swirling flows by Bruecker & Althaus (1995), Malkiel *et al.* (1996) and Mattner, Joubert & Chong (2002) and in the numerical simulations of Beran (1994), Lopez (1994) and Snyder & Spall (2000) for incompressible flows. The theoretical studies of Rusak and co-authors demonstrated the existence of a special mode of an axially symmetric disturbance that is not limited to the axial-Fourier mode and becomes unstable when the swirl ratio is above a certain critical level ω_1, which is the modified critical swirl of Benjamin (1962) due to pipe length. This instability mechanism is a result of the interaction between flow perturbations that are driven upstream by the swirl and the relatively fixed flow conditions at the pipe inlet. The studies also clarified the relationship between this instability mode, the axisymmetric vortex breakdown process, and the evolution to lower energy and stable breakdown states in high-Reynolds-number vortex flows.

In a recent paper, Rusak & Lee (2002) studied the effect of compressibility on the critical swirl level for breakdown of subsonic vortex flows in a straight circular pipe of finite length. This work extended the critical-state concept of Benjamin (1962) to include the influence of Mach number on the flow behaviour. The analysis was based

on a linearized version of the equations for the motion of a steady axisymmetric inviscid and compressible swirling flow of a prefect gas. The relationships between the velocity, density, temperature and pressure perturbations to a base columnar flow state were derived. An eigenvalue problem was formulated to determine the first critical level of swirl at which a special mode of a non-columnar small disturbance may appear on the base flow. It was found that when the characteristic Mach number of the base flow tends to zero the eigenvalue problem and ω_1 are the same as defined by Wang & Rusak (1996a, 1997a) in their study of incompressible swirling flows in pipes. As the characteristic Mach number is increased, ω_1 increases and the flow perturbation expands in the radial direction. As the Mach number approaches a certain limit value related to the core size of the vortex, ω_1 reaches very large values and becomes singular. These results indicated that the axisymmetric breakdown of high-Reynolds-number compressible vortex flows may be delayed to higher levels of the swirl ratio with the increase of the flow Mach number. This is similar to results found in the numerical simulations of Melville (1996) and Herrada *et al.* (2000).

We analyse in this paper the linear stability of a compressible inviscid axisymmetric and rotating columnar flow of a perfect gas in a finite-length pipe. In §2, we assume the physical model used in the works of Rusak and co-authors. We formulate a well-posed model of the unsteady motion of swirling flows with boundary conditions similar to those used in the steady compressible analysis of Rusak & Lee (2002) and in the incompressible flow analyses of Wang & Rusak (1996a, 1997a, b). We derive a linearized set of equations for the development of infinitesimal axially symmetric disturbances imposed on a base compressible rotating columnar flow. Then, we introduce a general mode of axisymmetric disturbance and obtain an eigenvalue problem (§3). We demonstrate that the critical level of swirl ω_1 defined by Rusak & Lee (2002) is a point of exchange of stability for any swirling flow in a finite-length pipe (§4). When the flow is supercritical, we find an asymptotically stable mode of axisymmetric disturbance and when the flow is subcritical we find an unstable mode of axisymmetric disturbance. The results shed more light on the effect of compressibility on the transition to axisymmetric breakdown (§5).

The present work focuses on the stability of compressible vortex flows. It should be clarified that the thermodynamics of vortex flows is always a matter of difficulty. The interaction between the velocity and thermodynamic properties is complicated and governed by, in addition to the momentum equations, the energy and state equations. Even the continuity and momentum equations contain changes of density that are related to the velocity perturbations. Moreover, the choice of boundary conditions in the compressible flow case, specifically the inlet thermodynamic conditions, is not unique and a certain model has to be assumed, for example, the inlet temperature profile is fixed. As a result, the stability problem in the compressible case is more involved than that in the incompressible case and requires a more careful and detailed study. The generalization of results for compressible flows is not simple or trivial. In fact, unlike the incompressible flow stability study of Wang & Rusak (1996a) where the perturbation equations reduce to one stability equation, the present work shows that the perturbation equations reduce to two stability equations that cannot be further simplified. Also, the linearized inlet conditions are more complex and affected by Mach number.

2. Mathematical model

An unsteady compressible non-heat conducting inviscid and axisymmetric swirling flow of a perfect gas is considered in a finite-length pipe of radius $\bar{r}_t$. The pipe

centreline is the $\bar{x}$-axis where $0 \leqslant \bar{x} \leqslant x_0 \bar{r}_t$ and the radial distance is $\bar{r}$ where $0 \leqslant \bar{r} \leqslant \bar{r}_t$. The flow thermodynamic properties are given by the equation of state:

$$\bar{P} = \bar{\rho} R \bar{T}, \tag{1}$$

where $\bar{P}$, $\bar{\rho}$ and $\bar{T}$ are the pressure, density, and temperature, respectively, and R is the specific gas constant. The compressible flow dynamics (where time is $\bar{t}$) is described by the unsteady and axisymmetric continuity, momentum and energy equations

$$\bar{\rho}_{\bar{t}} + (\bar{\rho}\bar{u})_{\bar{r}} + \frac{\bar{\rho}\bar{u}}{\bar{r}} + (\bar{\rho}\bar{w})_{\bar{x}} = 0, \tag{2}$$

$$\bar{\rho}\left(\bar{u}_{\bar{t}} + \bar{u}\bar{u}_{\bar{r}} + \bar{w}\bar{u}_{\bar{x}} - \frac{\bar{v}^2}{\bar{r}}\right) = -\bar{P}_{\bar{r}}, \tag{3}$$

$$\bar{v}_{\bar{t}} + \bar{u}\bar{v}_{\bar{r}} + \bar{w}\bar{v}_{\bar{x}} + \frac{\bar{u}\bar{v}}{\bar{r}} = 0, \tag{4}$$

$$\bar{\rho}(\bar{w}_{\bar{t}} + \bar{u}\bar{w}_{\bar{r}} + \bar{w}\bar{w}_{\bar{x}}) = -\bar{P}_{\bar{x}}, \tag{5}$$

$$\bar{\rho}C_p(\bar{T}_{\bar{t}} + \bar{u}\bar{T}_{\bar{r}} + \bar{w}\bar{T}_{\bar{x}}) - (\bar{P}_{\bar{t}} + \bar{u}\bar{P}_{\bar{r}} + \bar{w}\bar{P}_{\bar{x}}) = 0. \tag{6}$$

These equations construct the relationship between the thermodynamic properties and the radial, circumferential, and axial velocity components $\bar{u}$, $\bar{v}$ and $\bar{w}$, respectively. Also, C_p is the gas specific heat at a constant pressure process and is assumed constant, $C_p = \gamma R/(\gamma - 1)$ where γ is the ratio of specific heats of the perfect gas (for air at temperatures below 300 K, $\gamma = 1.4$, see Thompson 1988, p. 640).

We study the flow dynamics in the finite-length pipe under the following boundary conditions. We assume a physical model of the problem similar to that of Rusak and co-authors described in §1. For all $\bar{t}$, we set the symmetry conditions along the pipe centreline $\bar{r} = 0$

$$\bar{u}(\bar{t}, \bar{x}, 0) = 0, \ \bar{v}(\bar{t}, \bar{x}, 0) = 0, \ \bar{w}_{\bar{r}}(\bar{t}, \bar{x}, 0) = 0, \ \bar{T}_{\bar{r}}(\bar{t}, \bar{x}, 0) = 0, \ \bar{P}_{\bar{r}}(\bar{t}, \bar{x}, 0) = 0, \tag{7}$$

for $0 \leqslant \bar{x} \leqslant x_0 \bar{r}_t$. Along the pipe wall $\bar{r} = \bar{r}_t$, the normal (radial) velocity component vanishes for all $\bar{t}$, i.e.

$$\bar{u}(\bar{t}, \bar{x}, \bar{r}_t) = 0, \tag{8}$$

for $0 \leqslant \bar{x} \leqslant x_0 \bar{r}_t$. At the pipe inlet $\bar{x} = 0$, we prescribe a vortex state that is generated in front of the pipe and given for all $\bar{t}$ by

$$\bar{w}(\bar{t}, 0, \bar{r}) = \overline{U_0} w_0\left(\frac{\bar{r}}{\bar{r}_t}\right), \quad \bar{v}(\bar{t}, 0, \bar{r}) = \omega \overline{U_0} v_0\left(\frac{\bar{r}}{\bar{r}_t}\right),$$

$$\bar{\eta}(\bar{t}, 0, \bar{r}) = \frac{\overline{U_0}}{\bar{r}_t} \bar{\eta}_0\left(\frac{\bar{r}}{\bar{r}_t}\right), \quad \bar{T}(\bar{t}, 0, \bar{r}) = \bar{T}_0 T_0\left(\frac{\bar{r}}{\bar{r}_t}\right), \tag{9}$$

for $0 \leqslant \bar{r} \leqslant \bar{r}_t$. Here, $\bar{\eta} = \bar{u}_{\bar{x}} - \bar{w}_{\bar{r}}$ is the azimuthal vorticity. Also, $\overline{U_0}$ is the axial speed at the inlet centreline, ω is the swirl ratio of the incoming flow, and $\bar{T}_0$ is the temperature at the inlet centreline. The inlet flow is characterized by a Mach number $M_0 = \overline{U_0}/\bar{a}_0$ where $\bar{a}_0$ is the isentropic speed of sound at the inlet centreline, $\bar{a}_0 = (\gamma R \bar{T}_0)^{1/2}$. The given functions w_0, v_0, η_0, T_0 are independent of one another or of the Mach number and fully define the compressible flow at the inlet. In the present model, we use the temperature profile T_0 to describe the thermodynamic conditions at the inlet. The pressure and density at the inlet can be determined at every Mach number from the flow equations. Note that $w_{0\bar{r}}(0) = 0$, $v_0(0) = 0$ and $T_{0\bar{r}}(0) = 0$ should be used for symmetry at the inlet centreline. We also consider in the present study the nominal

case where for all $\bar{t}$ there is a zero axial gradient of the radial speed along the pipe inlet and the inlet azimuthal vorticity is fixed, i.e. for all $\bar{t}$:

$$\bar{\eta}_0 = -\bar{w}_{0\bar{r}} \quad \text{or} \quad \bar{u}_{\bar{x}}(\bar{t}, 0, \bar{r}) = 0 \quad \text{for every} \quad 0 \leqslant \bar{r} \leqslant \bar{r}_t. \tag{10}$$

Also, we assume at the inlet centreline that the pressure is fixed for all $\bar{t}$, i.e.

$$\bar{P}(\bar{t}, 0, 0) = \bar{P}_0 \tag{11}$$

is given. No radial velocity and non-reflective conditions on the thermodynamic properties are assumed along the pipe outlet at $\bar{x} = x_0 \bar{r}_t$, i.e. for all $\bar{t}$:

$$\bar{u}(\bar{t}, x_0\bar{r}_t, \bar{r}) = 0, \quad \bar{P}_{\bar{t}}(\bar{t}, x_0\bar{r}_t, \bar{r}) + \bar{w}\bar{P}_{\bar{x}}(\bar{t}, x_0\bar{r}_t, \bar{r}) = 0 \quad \text{for} \quad 0 \leqslant \bar{r} \leqslant \bar{r}_t. \tag{12}$$

These conditions are compatible with the fully developed flow conditions at the pipe outlet in the incompressible flow problem and are typically used in the study of compressible flow problems (see Thompson 1987). The boundary conditions (7)–(12) are similar to those used in compressible flow simulations by Melville (1996), Tromp & Beran (1996, 1997) and Herrada *et al.* (2000).

Equations (1)–(6) with boundary conditions (7)–(12) formulate a well-defined problem to describe the inviscid dynamics of a compressible axisymmetric rotating flow in a finite-length pipe. We use these equations to study the stability of a columnar vortex state.

3. Perturbation equations

We consider a base steady, swirling and columnar flow solution of (1)–(12) where for every Mach number M_0 and swirl level ω and for all $\bar{t}$ and $0 \leqslant \bar{x} \leqslant x_0 \bar{r}_t$

$$\left.\begin{aligned}
&\bar{w}(\bar{t}, \bar{x}, \bar{r}) = \overline{U_0} w_0\left(\frac{\bar{r}}{\bar{r}_t}\right), \ \bar{v}(\bar{t}, \bar{x}, \bar{r}) = \omega\overline{U_0} v_0\left(\frac{\bar{r}}{\bar{r}_t}\right), \ \bar{u}(\bar{t}, \bar{x}, \bar{r}) = 0, \\[6pt]
&\bar{T}(\bar{t}, \bar{x}, \bar{r}) = \bar{T}_0 T_0\left(\frac{\bar{r}}{\bar{r}_t}\right), \\[6pt]
&\bar{P}(\bar{t}, \bar{x}, \bar{r}) = \bar{P}_0 P_0\left(\frac{\bar{r}}{\bar{r}_t}\right), \ P_0\left(\frac{\bar{r}}{\bar{r}_t}\right) = \exp\left(\gamma M_0^2 \omega^2 \int_0^{\bar{r}/\bar{r}_t} \frac{v_0^2(\bar{r}^*/\bar{r}_t)}{(\bar{r}^*/\bar{r}_t)T_0(\bar{r}^*/\bar{r}_t)} \, d\left(\frac{\bar{r}^*}{\bar{r}_t}\right)\right) \\[6pt]
&\bar{\rho}(\bar{t}, \bar{x}, \bar{r}) = \bar{\rho}_0 \rho_0\left(\frac{\bar{r}}{\bar{r}_t}\right), \ \rho_0\left(\frac{\bar{r}}{\bar{r}_t}\right) = P_0\left(\frac{\bar{r}}{\bar{r}_t}\right) \Big/ T_0\left(\frac{\bar{r}}{\bar{r}_t}\right), \ \bar{P}_0 = \bar{\rho}_0 R\bar{T}_0.
\end{aligned}\right\} \tag{13}$$

The exponential dependence of P_0 is found from substituting (13) into (1) and (3) and using (1) to express $\bar{\rho}$ in terms of $\bar{P}$ and $\bar{T}$. This results in an equation for P_0: $P_{0\bar{r}}/P_0 = \gamma M_0^2 \omega^2 v_0^2/(\bar{r}T_0)$, the solution which is given in (13). Note that in the columnar flow state, only the pressure and density depend on Mach number.

We use $t = (\overline{U_0}/\bar{r}_t)\bar{t}$, $r = \bar{r}/\bar{r}_t$, and $x = \bar{x}/\bar{r}_t$ as non-dimensional variables. To study the stability of the base vortex flow we introduce infinitesimal perturbations to the base flow variables in the form

$$\left.\begin{aligned}
&\bar{\rho} = \bar{\rho}_0\big(\rho_0(r) + \gamma M_0^2 \epsilon \rho_1(t, x, r) + \ldots\big), \\
&\bar{T} = \bar{T}_0\big(T_0(r) + \gamma M_0^2 \epsilon T_1(t, x, r) + \ldots\big), \\
&\bar{P} = \bar{P}_0\big(P_0(r) + \gamma M_0^2 \epsilon P_1(t, x, r) + \ldots\big), \\
&\bar{w} = \overline{U_0}(w_0(r) + \epsilon w_1(t, x, r) + \ldots), \\
&\bar{u} = \overline{U_0}(\epsilon u_1(t, x, r) + \ldots), \\
&\bar{v} = \overline{U_0}(\omega v_0(r) + \epsilon v_1(t, x, r) + \ldots),
\end{aligned}\right\} \tag{14}$$

where $|\epsilon| \ll 1$ and $\rho_1, T_1, P_1, u_1, v_1, w_1$ are the unsteady disturbances. On substituting these asymptotic expressions into (1)–(12) and neglecting second-order terms, we then obtain the base flow relations and the unsteady linearized equations of motion of the swirling flow:

equation of state

$$O(1) : P_0 = \rho_0 T_0, \tag{15}$$

$$O(\epsilon) : P_1 = \rho_1 T_0 + \rho_0 T_1; \tag{16}$$

continuity equation

$$O(\epsilon) : \gamma M_0^2 \rho_{1t} + \frac{1}{r}(r\rho_0 u_1)_r + \left(\rho_0 w_1 + \gamma M_0^2 \rho_1 w_0\right)_x = 0; \tag{17}$$

r-momentum equation

$$O(1) : P_{0r} = \gamma M_0^2 \rho_0 \omega^2 \frac{v_0^2}{r}, \tag{18}$$

$$O(\epsilon) : \rho_0 u_{1t} + \rho_0 w_0 u_{1x} - \frac{2}{r}\omega v_0 \rho_0 v_1 - \gamma M_0^2 \omega^2 \frac{v_0^2}{r} \rho_1 = -P_{1r}; \tag{19}$$

x-momentum equation

$$O(\epsilon) : \rho_0 w_{1t} + \rho_0 w_{0r} u_1 + \rho_0 w_0 w_{1x} = -P_{1x}; \tag{20}$$

θ-momentum equation

$$O(\epsilon) : v_{1t} + \omega \frac{1}{r}(rv_0)_r u_1 + w_0 v_{1x} = 0; \tag{21}$$

energy equation

$$O(\epsilon) : \frac{\gamma}{\gamma - 1}\left[\rho_0 u_1 T_{0r} + \gamma M_0^2(\rho_0 T_{1t} + \rho_0 w_0 T_{1x})\right] - \left[u_1 P_{0r} + \gamma M_0^2(P_{1t} + w_0 P_{1x})\right] = 0; \tag{22}$$

where the relation $C_p/R = \gamma/(\gamma - 1)$ has been used. According to (7)–(12) and asymptotic expansions (14), equations (15)–(22) are subjected to the following boundary conditions. For all t, along the pipe centreline $r = 0$:

$$u_1(t, x, 0) = v_1(t, x, 0) = w_{1r}(t, x, 0) = T_{1r}(t, x, 0) = P_{1r}(t, x, 0) = 0 \quad \text{for} \quad 0 \leqslant x \leqslant x_0, \tag{23}$$

along the pipe wall $r = 1$:

$$u_1(t, x, 1) = 0 \quad \text{for} \quad 0 \leqslant x \leqslant x_0, \tag{24}$$

and at the pipe inlet $x = 0$:

$$w_1(t, 0, r) = v_1(t, 0, r) = u_{1x}(t, 0, r) = T_1(t, 0, r) = 0 \quad \text{for} \quad 0 \leqslant r \leqslant 1. \tag{25}$$

Note that (16), (19) and (25) result for all t in:

$$P_1(t, 0, r) = \rho_1(t, 0, r)T_0(r),$$

$$\rho_0(r)u_{1t}(t, 0, r) - \gamma M_0^2 \omega^2 \frac{v_0^2(r)}{r T_0(r)} P_1(t, 0, r) = -P_{1r}(t, 0, r) \quad \text{for} \quad 0 \leqslant r \leqslant 1 \tag{26}$$

with $P_1(t, 0, 0) = 0$. At the pipe outlet $x = x_0$, we set for all t:

$$u_1(t, x_0, r) = 0, \quad P_{1t}(t, x_0, r) + w_0(r)P_{1x}(t, x_0, r) = 0 \quad \text{for} \quad 0 \leqslant r \leqslant 1. \tag{27}$$

We define $y = r^2/2$ where $0 \leqslant y \leqslant 1/2$. From the linearized continuity equation (17), a function $\psi_1(t, x, y)$ can be defined such that:

$$\rho_0 u_1 = -\frac{\psi_{1x}}{\sqrt{2y}}, \quad \rho_0 w_1 = \psi_{1y} - \gamma M_0^2 \left(w_0 \rho_1 + \int_0^x \rho_{1t}(t, x', y) \, dx' \right). \tag{28}$$

To fix the function $\psi_1(t, x, y)$, we set for all t: $\psi_1(t, 0, 0) = 0$.

Let $K = rv$ be the circulation function where $K = \omega K_0(y) + \epsilon K_1 + \ldots$, $K_0(y) = (2y)^{1/2} v_0$ is the base flow circulation function, and $K_1(t, x, y)$ is the circulation unsteady disturbance. The linearized θ-momentum equation (21) can be changed to:

$$K_{1t} + \omega \sqrt{2y} u_1 K_{0y} + w_0 K_{1x} = 0. \tag{29}$$

Elimination of pressure from (19) and (20) by cross-differentiation in terms of x and y, respectively, followed by subtraction gives a relationship between ψ_1, K_{1x} and ρ_1. Solving it for K_{1x} and substituting in (29) results in additional expression for K_{1t}. Elimination of K_1 by cross-differentiation in terms of t and x, respectively, followed by subtraction, multiplying by $\omega K_0 \rho_0 / (2y^2 w_0)$, and differentiation with respect to x gives (as shown in Appendix A)†,

$$2 \left(\frac{\psi_{1xx}}{2y} + \psi_{1yy} \right)_{xxt} + \frac{1}{w_0} \left(\frac{\psi_{1xx}}{2y} + \psi_{1yy} \right)_{xtt} + w_0 \left(\frac{\psi_{1xx}}{2y} + \psi_{1yy} \right)_{xxx}$$

$$+ \left(\frac{\omega^2 K_0 K_{0y}}{2y^2 w_0} - w_{0yy} \right) \psi_{1xxx} - \frac{w_{0yy}}{w_0} \psi_{1xxt}$$

$$= -\gamma M_0^2 \left[\frac{\omega^2 K_0^2}{4y^2} \left(\rho_{1xxx} + \frac{\rho_{1xxt}}{w_0} \right) - 4 w_{0y} \rho_{1xxt} - 3 \rho_{1xytt} - 3 w_0 \rho_{1xxyt} \right.$$

$$\left. - \frac{1}{w_0} \rho_{1yttt} - \frac{2 w_{0y}}{w_0} \rho_{1xtt} - 2 w_0 w_{0y} \rho_{1xxx} - w_0^2 \rho_{1xxxy} \right]. \tag{30}$$

Equation (30) presents one relationship between ψ_1 and ρ_1. Another relationship between these disturbances is now found from the linearized state and energy equations (16) and (22). Differentiating (22) with respect to x, substituting $\rho_0 T_1 = P_1 - \rho_1 T_0$, using (20) to express P_{1xt} and P_{1xx}, multiplying by $-1/w_0$, and differentiating with respect to x gives (as shown in Appendix A),

$$\gamma M_0^2 \left[\left(\frac{T_0}{w_0} - 3 M_0^2 w_0 \right) \rho_{1xxt} + (T_0 - M_0^2 w_0^2) \rho_{1xxx} - 3 M_0^2 \rho_{1xtt} - \frac{M_0^2}{w_0} \rho_{1ttt} \right]$$

$$= \left(M_0^2 w_{0y} - \frac{T_{0y}}{w_0} + \frac{\gamma - 1}{\gamma} \frac{P_{0y}}{\rho_0 w_0} \right) \psi_{1xxx} - M_0^2 w_0 \psi_{1xxxy} - \frac{M_0^2}{w_0} \psi_{1xytt}$$

$$+ M_0^2 \frac{w_{0y}}{w_0} \psi_{1xxt} - 2 M_0^2 \psi_{1xxyt}. \tag{31}$$

Equations (30) and (31) describe the linearized dynamics of the disturbances ψ_1 and ρ_1. For a well-defined problem, these equations must be subjected for all t to two conditions on ψ_1 and no condition on ρ_1 along the pipe centreline and wall and five conditions on ψ_1 and three conditions on ρ_1 along the pipe inlet and outlet. These conditions are derived from the boundary conditions (23)–(27), as follows.

---

† Appendices A–D are available as a supplement to the online version of this paper or from the authors or the JFM Editorial office.

From (23) and (24), for all t, along the pipe centreline $r = 0$:

$$\psi_1(t, x, 0) = \psi_1(t, 0, 0) = 0 \quad \text{for} \quad 0 \leqslant x \leqslant x_0, \tag{32}$$

and along the pipe wall $r = 1$:

$$\psi_1(t, x, 1/2) = \psi_1(t, 0, 1/2) \quad \text{for} \quad 0 \leqslant x \leqslant x_0, \tag{33}$$

where $\psi_1(t, 0, 1/2)$ has to be determined. The inlet conditions (25) show that for all t

$$\psi_{1xx}(t, 0, y) = 0 \quad \text{for} \quad 0 \leqslant y \leqslant 1/2. \tag{34}$$

Also, from (25), (26) and (28), we find along the pipe inlet that for all t and $0 \leqslant y \leqslant 1/2$

$$\left. \begin{array}{l} \gamma M_0^2 w_0 \rho_1(t, 0, y) = \psi_{1y}(t, 0, y), \\[2mm] \dfrac{\psi_{1xt}(t, 0, y)}{2y} = T_0 \rho_{1y}(t, 0, y) + T_{0y} \rho_1(t, 0, y) - \gamma M_0^2 \omega^2 \dfrac{K_0^2}{4y^2} \rho_1(t, 0, y), \end{array} \right\} \tag{35}$$

$$\text{with conditions:} \quad \psi_1(t, 0, 0) = 0, \quad \rho_1(t, 0, 0) = 0.$$

Conditions in (35) result for all t and $0 \leqslant y \leqslant 1/2$ in

$$\left(\frac{T_0}{w_0} \psi_{1y}(t, 0, y) \right)_y = \gamma M_0^2 \left(\frac{\psi_{1xt}(t, 0, y)}{2y} + \omega^2 \frac{K_0^2}{4y^2 w_0} \psi_{1y}(t, 0, y) \right), \tag{36}$$

$$\text{with conditions:} \quad \psi_1(t, 0, 0) = \psi_{1y}(t, 0, 0) = 0,$$

which can replace the second condition in (35). Condition (36) describes a certain relationship between ψ_1 and ψ_{1x} at the pipe inlet. Note that in the stability problem of an incompressible vortex flow (where $M_0 = 0$) or in the problem of the linearized steady compressible vortex flow (where $\psi_{1xt} = 0$), the condition (36) reduces to $\psi_1(t, 0, y) = 0$ along the pipe inlet $0 \leqslant y \leqslant 1/2$ that was used in the analyses of Wang & Rusak (1996a) and Rusak & Lee (2002). The present condition (36) for the stability of the compressible vortex flow adds a special difficulty that was not present in any of the previous studies, i.e. the distribution of $\psi_1(t, 0, y)$ for $0 \leqslant y \leqslant 1/2$ has to be determined as part of the solution of the flow linearized dynamics.

Three additional inlet conditions result from (25) and (A 2), (A 3) and (A 6), i.e. for all t and $0 \leqslant y \leqslant 1/2$:

$$\frac{\psi_{1xxx}(t, 0, y)}{2y} + \psi_{1xyy}(t, 0, y) + \left(\frac{\omega^2 K_0 K_{0y}}{2y^2 w_0^2} - \frac{w_{0yy}}{w_0} \right) \psi_{1x}(t, 0, y) + \frac{\psi_{1yyt}(t, 0, y)}{w_0}$$

$$= -\gamma M_0^2 \left[\left(\frac{\omega^2 K_0^2}{4y^2 w_0} - 2w_{0y} \right) \rho_{1x}(t, 0, y) - w_0 \rho_{1xy}(t, 0, y) \right.$$

$$\left. - 2 \frac{w_{0y}}{w_0} \rho_{1t}(t, 0, y) - 2\rho_{1yt}(t, 0, y) \right], \tag{37}$$

$$\frac{\psi_{1xxxt}(t, 0, y)}{y w_0} + \frac{2\psi_{1xyyt}(t, 0, y)}{w_0} + \frac{1}{w_0^2} \psi_{1yytt}(t, 0, y) + \frac{\psi_{1xxxx}(t, 0, y)}{2y} - \frac{w_{0yy}}{w_0^2} \psi_{1xt}(t, 0, y)$$

$$= -\frac{\gamma M_0^2}{w_0} \left[\frac{\omega^2 K_0^2}{4y^2} \left(\rho_{1xx}(t, 0, y) + \frac{\rho_{1xt}(t, 0, y)}{w_0} \right) - 4w_{0y} \rho_{1xt}(t, 0, y) - 3\rho_{1ytt}(t, 0, y) \right.$$

$$\left. - 3w_0 \rho_{1xyt}(t, 0, y) - \frac{2w_{0y}}{w_0} \rho_{1tt}(t, 0, y) - 2w_0 w_{0y} \rho_{1xx}(t, 0, y) - w_0^2 \rho_{1xxy}(t, 0, y) \right], \tag{38}$$

$$\gamma \left[\left(\frac{T_0}{w_0} - 3M_0^2 w_0 \right) \rho_{1xt}(t, 0, y) + (T_0 - M_0^2 w_0^2) \rho_{1xx}(t, 0, y) - 3M_0^2 \rho_{1tt}(t, 0, y) \right]$$

$$= \frac{w_{0y}}{w_0} \psi_{1xt}(t, 0, y) - \frac{1}{w_0} \psi_{1ytt}(t, 0, y) - 2\psi_{1xyt}(t, 0, y). \quad (39)$$

From (27), the outlet conditions for all t and $0 \leqslant y \leqslant 1/2$ are:

$$\psi_{1x}(t, x_0, y) = 0, \quad (40)$$

$$\rho_{1t}(t, x_0, y) + w_0 \rho_{1x}(t, x_0, y) = 0. \quad (41)$$

In summary, (30) and (31) are subjected to (32) and (33) which describe the two conditions on ψ_1 along the pipe centreline and wall, (34), (36), (37), (38) and (40) which are the five conditions on ψ_1 along the pipe inlet and outlet, and (35), (39) and (41) which are the three conditions on ρ_1 along the pipe inlet and outlet.

4. Mode analysis

We consider a suitable general mode analysis of (30), (31) and (32)–(41) of the form

$$\psi_1 = \tilde{\phi}(x, y) e^{\sigma t}, \quad \rho_1 = \tilde{\rho}(x, y) e^{\sigma t}. \quad (42)$$

Here, in the general case, the rate σ is a complex number and $\tilde{\phi}$ and $\tilde{\rho}$ are complex functions. Substituting (42) into (30) and (31) gives two equations for the solution of $\tilde{\phi}$ and $\tilde{\rho}$:

$$2\sigma \left(\frac{\tilde{\phi}_{xx}}{2y} + \tilde{\phi}_{yy} \right)_{xx} + \frac{\sigma^2}{w_0} \left(\frac{\tilde{\phi}_{xx}}{2y} + \tilde{\phi}_{yy} \right)_x + w_0 \left(\frac{\tilde{\phi}_{xx}}{2y} + \tilde{\phi}_{yy} \right)_{xxx}$$

$$+ \left(\frac{\omega^2 K_0 K_{0y}}{2y^2 w_0} - w_{0yy} \right) \tilde{\phi}_{xxx} - \sigma \frac{w_{0yy}}{w_0} \tilde{\phi}_{xx}$$

$$= -\gamma M_0^2 \left[\frac{\omega^2 K_0^2}{4y^2} \left(\tilde{\rho}_{xxx} + \sigma \frac{\tilde{\rho}_{xx}}{w_0} \right) - 4\sigma w_{0y} \tilde{\rho}_{xx} - 3\sigma^2 \tilde{\rho}_{xy} \right.$$

$$\left. - 3\sigma w_0 \tilde{\rho}_{xxy} - \sigma^3 \frac{\tilde{\rho}_y}{w_0} - \sigma^2 \frac{2w_{0y}}{w_0} \tilde{\rho}_x - 2w_0 w_{0y} \tilde{\rho}_{xxx} - w_0^2 \tilde{\rho}_{xxxy} \right] = 0, \quad (43)$$

$$\gamma M_0^2 \left[\sigma \left(\frac{T_0}{w_0} - 3M_0^2 w_0 \right) \tilde{\rho}_{xx} + (T_0 - M_0^2 w_0^2) \tilde{\rho}_{xxx} - 3\sigma^2 M_0^2 \tilde{\rho}_x - \sigma^3 \frac{M_0^2}{w_0} \tilde{\rho} \right]$$

$$= \left(M_0^2 w_{0y} - \frac{T_{0y}}{w_0} + \frac{\gamma - 1}{\gamma} \frac{P_{0y}}{\rho_0 w_0} \right) \tilde{\phi}_{xxx} - M_0^2 w_0 \tilde{\phi}_{xxxy}$$

$$- \sigma^2 \frac{M_0^2}{w_0} \tilde{\phi}_{xy} + \sigma M_0^2 \frac{w_{0y}}{w_0} \tilde{\phi}_{xx} - 2\sigma M_0^2 \tilde{\phi}_{xxy}. \quad (44)$$

The boundary conditions for these equations are derived from (32)–(41) by replacing ψ_1 with $\tilde{\phi}$ and derivatives with t by respective powers of σ (as shown in Appendix B).

Equations (43) and (44) constitute an eigenvalue problem for the solution of σ $\tilde{\phi}$ and $\tilde{\rho}$ for all swirl levels ω. For each ω the problem has an infinite number of eigenvalues σ.

Note that for the case where $\sigma = 0$, the inlet conditions (B 3) and (B 4) can be solved and give $\tilde{\phi}(0, y) = 0$ and $\tilde{\rho}(0, y) = 0$ for $0 \leqslant y \leqslant 1/2$. We use this result in §4.1 when we study the case where $\sigma = 0$ (a neutral mode).

Reduction of (43) and (44) into one equation for $\tilde{\phi}$ is complicated and requires the use of higher-order derivatives in x and y. Since we are specifically interested

in investigating the stability of the base compressible vortex flow around its critical state, we use the following asymptotic mode analysis.

4.1. *The neutral mode*

We first concentrate on the case where $\sigma = 0$ (a neutral mode). Then, the system (43) and (44) reduces to

$$\left[\frac{\tilde{\phi}_{xx}}{2y} + \tilde{\phi}_{yy} + \left(\frac{\omega^2 K_0 K_{0y}}{2y^2 w_0^2} - \frac{w_{0yy}}{w_0}\right)\tilde{\phi} + \gamma M_0^2\left(\frac{\omega^2 K_0^2}{4y^2 w_0}\tilde{\rho} - 2w_{0y}\tilde{\rho} - w_0\tilde{\rho}_y\right)\right]_{xxx} = 0, \quad (45)$$

$$\gamma M_0^2 \tilde{\rho}_{xxx} = \frac{1}{\left(T_0 - M_0^2 w_0^2\right)}\left[\left(M_0^2 w_{0y} - \frac{T_{0y}}{w_0} + \frac{\gamma - 1}{\gamma}\frac{P_{0y}}{\rho_0 w_0}\right)\tilde{\phi} - M_0^2 w_0\tilde{\phi}_y\right]_{xxx}, \quad (46)$$

with boundary conditions

$$\tilde{\phi}(x, 0) = 0, \quad \tilde{\phi}(x, 1/2) = \tilde{\phi}(0, 1/2) = 0, \quad (47)$$

for $0 \leqslant x \leqslant x_0$ and

$$\tilde{\phi}(0, y) = 0, \quad \tilde{\phi}_{xx}(0, y) = 0, \quad \tilde{\phi}_{xxxx}(0, y) = 0, \quad \tilde{\phi}_x(x_0, y) = 0, \quad (48)$$

$$\frac{\tilde{\phi}_{xxx}(0, y)}{2y} + \tilde{\phi}_{xyy}(0, y) + \left(\frac{\omega^2 K_0 K_{0y}}{2y^2 w_0^2} - \frac{w_{0yy}}{w_0}\right)\tilde{\phi}_x(0, y)$$

$$= -\gamma M_0^2\left[\left(\frac{\omega^2 K_0^2}{4y^2 w_0} - 2w_{0y}\right)\tilde{\rho}_x(0, y) - w_0\tilde{\rho}_{xy}(0, y)\right], \quad (49)$$

$$\tilde{\rho}(0, y) = 0, \quad \tilde{\rho}_{xx}(0, y) = 0, \quad \tilde{\rho}_x(x_0, y) = 0 \quad (50)$$

for $0 \leqslant y \leqslant 1/2$. Substituting (46) into (45) followed by three integrations with respect to x and using (47)–(50) gives

$$\mathcal{L}(\tilde{\phi}; \Omega) \equiv \tilde{\phi}_{yy} + \frac{\tilde{\phi}_{xx}}{2y}\frac{T_0 - M_0^2 w_0^2}{T_0} + \tilde{\phi}_y Q(y; \Omega) + \tilde{\phi}R(y; \Omega) = 0 \quad (51)$$

where

$$Q(y; \Omega) = -\frac{\gamma M_0^2 \Omega K_0^2}{4y^2 T_0} + \frac{\left(T_0 - 2M_0^2 w_0^2\right)T_{0y} + 2M_0^2 w_0 w_{0y} T_0}{\left(T_0 - M_0^2 w_0^2\right)T_0},$$

$$R(y; \Omega) = \left(\frac{\Omega K_0 K_{0y}}{2y^2 w_0^2} - \frac{w_{0yy}}{w_0}\right)\frac{T_0 - M_0^2 w_0^2}{T_0}$$

$$+ \frac{\Omega K_0^2}{4y^2 w_0^2 T_0}\left(M_0^2 w_0 w_{0y} - T_{0y} + (\gamma - 1)M_0^2\frac{\Omega K_0^2}{4y^2}\right)$$

$$- \frac{T_0 - M_0^2 w_0^2}{w_0 T_0}\left(w_0\frac{M_0^2 w_0 w_{0y} - T_{0y} + (\gamma - 1)M_0^2 \Omega K_0^2/(4y^2)}{T_0 - M_0^2 w_0^2}\right)_y$$

with boundary conditions

$$\tilde{\phi}(x, 0) = 0, \quad \tilde{\phi}(x, 1/2) = 0 \quad \text{for } 0 \leqslant x \leqslant x_0, \quad (52)$$

$$\tilde{\phi}(0, y) = 0, \quad \tilde{\phi}_x(x_0, y) = 0 \quad \text{for } 0 \leqslant y \leqslant 1/2. \quad (53)$$

Here, $\Omega = \omega^2$. Comparing (51)–(53) with equations (43)–(45) in Rusak & Lee (2002), we observe that when $\sigma = 0$, a neutrally stable mode of disturbance exists at the specific swirl level $\omega = \omega_1$ that has been defined in Rusak & Lee (2002) as 'the critical

swirl ratio for a compressible vortex flow in a finite-length pipe'. The solution of the eigenvalue problem (51)–(53) is

$$\tilde{\phi} = \psi_{1c}(x, y) = \Phi(y) \sin\left(\frac{\pi x}{2x_0}\right) \tag{54}$$

where Φ is the eigenfunction that corresponds to the critical state at the first eigenvalue $\Omega_1 = \omega_1^2$ and both are found from the solution of:

$$\Phi_{yy} + \Phi_y Q(y; \Omega_1) + \Phi R_1(y; \Omega_1) = 0, \tag{55}$$

where

$$R_1(y; \Omega_1) = R(y; \Omega_1) - \frac{\pi^2}{8yx_0^2} \frac{T_0 - M_0^2 w_0^2}{T_0},$$

with boundary conditions:

$$\Phi(0) = \Phi(1/2) = 0. \tag{56}$$

The corresponding critical density perturbation is

$$\tilde{\rho} = \rho_{1c}(x, y) = S(y) \sin\left(\frac{\pi x}{2x_0}\right), \tag{57}$$

where

$$S(y) = \frac{1}{\gamma M_0^2 w_0 (T_0 - M_0^2 w_0^2)} \left[\left(M_0^2 w_0 w_{0y} - T_{0y} + (\gamma - 1) M_0^2 \frac{\Omega_1 K_0^2}{4y^2} \right) \Phi - M_0^2 w_0^2 \Phi_y \right].$$

Results of calculations of the critical swirl ω_1 and the eigenfunction $\Phi(y)$ according to (55) and (56) for a solid-body rotation and for a Burgers vortex at various subsonic Mach numbers and vortex core radii are shown in Rusak & Lee (2002). Note that $\sigma = 0$ also occurs at higher eigenvalues $\omega_2, \omega_3, \ldots$ of the problem (55) and (56) which are greater than ω_1, but these are beyond the interest of the present analysis.

Note that, unlike the incompressible case, in the compressible case the problem (55)–(56) is not self-adjoint. The adjoint function of ψ_{1c} is given by:

$$\psi_{1c}^*(x, y) = \Phi^*(y) \sin\left(\frac{\pi x}{2x_0}\right), \tag{58}$$

where Φ^* is the adjoint eigenfunction that corresponds to the critical state at the first eigenvalue $\Omega_1 = \omega_1^2$ and is computed from the solution of:

$$\Phi_{yy}^* - \Phi_y^* Q(y; \Omega_1) + \Phi^* [R_1(y; \Omega_1) - Q_y(y; \Omega_1)] = 0, \tag{59}$$

with boundary conditions:

$$\Phi^*(0) = \Phi^*(1/2) = 0.$$

Figure 1 shows for various Mach numbers M_0 the computed critical function $\Phi(y)$ and its adjoint function $\Phi^*(y)$ for the case of a solid-body rotation where $w_0(y) = 1$, $v_0 = (2y)^{1/2}$, and $x_0 = 60$. It can be seen that the adjoint function Φ^* is close to the eigenfunction Φ when M_0 is sufficiently small ($0 \leqslant M_0 \leqslant 0.3$) but as M_0 increases the two functions are different.

4.2. Stability analysis around the critical state

In the previous section, we have shown that the critical state for a compressible vortex at the swirl level $\omega = \omega_1$ is also a state with a neutral mode of disturbance. We
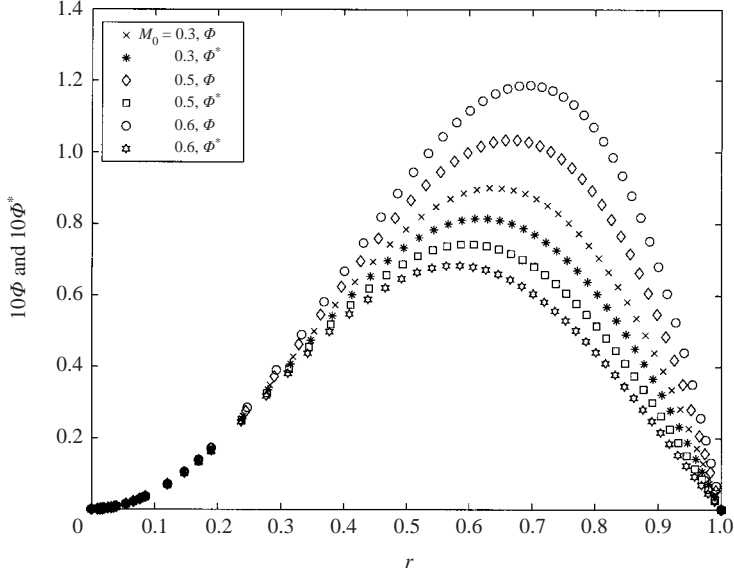
FIGURE 1. The computed critical function $\Phi(y)$ and its adjoint function $\Phi^*(y)$ for the case of a solid-body rotation in a pipe with $x_0 = 60$ at various Mach numbers.

study now the stability of the compressible vortex at swirl levels around ω_1 as it is described by (43) and (44). Let $\omega^2 = \Omega_1 + \Delta\Omega$. It is expected that as $\Delta\Omega \to 0$ also $\sigma = \sigma_R + i\sigma_I \to 0$. Here, i is the imaginary unit, σ_R and $i\sigma_I$ are the real and imaginary parts of σ, both are functions of $\Delta\Omega$ and tend to zero as $\Delta\Omega \to 0$.

We consider the following asymptotic expansions for $\tilde{\phi}$ and $\tilde{\rho}$ in the limit $\omega \to \omega_1$:

$$\left.\begin{aligned} \tilde{\phi} &= \psi_{1c}(x, y) + \epsilon_R \phi_R(x, y) + i\epsilon_I \phi_I(x, y) + \ldots, \\ \tilde{\rho} &= \rho_{1c}(x, y) + \epsilon_R \rho_R(x, y) + i\epsilon_I \rho_I(x, y) + \ldots. \end{aligned}\right\} \tag{60}$$

Here, ϵ_R, and ϵ_I are real functions of $\Delta\Omega$ and tend to zero as $\Delta\Omega \to 0$. The functions ϕ_R, ϕ_I, ρ_R and ρ_I are real functions. We first concentrate on the imaginary parts of (43) and (44). Collecting terms of the orders $\epsilon_I, \sigma_I, \epsilon_I\sigma_R, \epsilon_I\Delta\Omega$ and neglecting terms of the orders $O(\sigma_R^2, \sigma_I^2, \sigma_R\sigma_I, \sigma_I\epsilon_R, \sigma_I\Delta\Omega)$ and higher gives (as shown in Appendix C),

$$\epsilon_I[\mathscr{L}(\phi_I(x, y); \Omega_1) - \mathscr{L}(\phi_I(0, y); \Omega_1)] - \sigma_I \int_0^x \mathscr{L}_1[\psi_{1c}(x', y), \rho_{1c}(x', y); \Omega_1] \, dx'$$

$$+ \epsilon_I\sigma_R \int_0^x \mathscr{L}_2[\phi_I(x', y), \rho_I(x', y); \Omega_1] \, dx' + \epsilon_I\Delta\Omega[\mathscr{L}_3(\phi_I(x, y); \rho_I(x, y); \Omega_1)$$

$$- \mathscr{L}_3(\phi_I(0, y); \rho_I(0, y); \Omega_1)] = 0. \tag{61}$$

The functional $\mathscr{L}(\phi_I(x, y); \Omega_1)$ in (61) is the same as defined in (51). In the functional $\mathscr{L}(\phi_I(0, y); \Omega_1)$, the condition $\phi_{Ixx}(0, y) = 0$ is used. The functions $\mathscr{L}_1$, $\mathscr{L}_2$ and $\mathscr{L}_3$ in (61) can be presented by detailed expressions, but these are not needed here for the following calculation (details of $\mathscr{L}_1$ and $\mathscr{L}_3$ are given later in (64) and (65)). The multiplication of (61) by the adjoint function $\psi_{1c}^*(x, y)$ (given by (58)–(59)) and the

integration over the flow domain $0 \leqslant x \leqslant x_0$ and $0 \leqslant y \leqslant 1/2$ results in

$$
\epsilon_I \int_0^{x_0} \int_0^{1/2} [\mathscr{L}(\phi_I(x, y); \Omega_1) - \mathscr{L}(\phi_I(0, y); \Omega_1)] \, \psi_{1c}^*(x, y) \, \mathrm{d}y \, \mathrm{d}x
$$

$$
+ \sigma_I \int_0^{x_0} \int_0^{1/2} \left[\int_0^x \mathscr{L}_1(\psi_{1c}(x', y), \rho_{1c}(x', y); \Omega_1) \, \mathrm{d}x' \right] \psi_{1c}^*(x, y) \, \mathrm{d}y \, \mathrm{d}x
$$

$$
+ \epsilon_I \sigma_R \int_0^{x_0} \int_0^{1/2} \left[\int_0^x \mathscr{L}_2(\phi_I(x', y), \rho_I(x', y); \Omega_1) \, \mathrm{d}x' \right] \psi_{1c}^*(x, y) \, \mathrm{d}y \, \mathrm{d}x
$$

$$
+ \epsilon_I \Delta\Omega \int_0^{x_0} \int_0^{1/2} [\mathscr{L}_3(\phi_I(x, y), \rho_I(x, y); \Omega_1)
$$

$$
- \mathscr{L}_3(\phi_I(0, y), \rho_I(0, y); \Omega_1)] \psi_{1c}^*(x, y) \, \mathrm{d}y \, \mathrm{d}x = 0. \tag{62}
$$

Calculation shows that the first term in (62) vanishes. Therefore, we find from (62) that $\sigma_I = O(\epsilon_I \sigma_R, \epsilon_I \Delta\Omega)$. This means that $|\sigma_I| \ll |\sigma_R|$ and $|\sigma_I| \ll |\Delta\Omega|$. Moreover, this conclusion for the compressible flow case matches a similar result found in the stability analysis of incompressible flow by Wang & Rusak (1996*a*). Note that the stability analysis of Gallaire & Chomaz (2001), who extended the work of Wang & Rusak (1996*a*), shows by numerical computations of the incompressible flow problem that $\sigma_I = 0$ and $\epsilon_I = 0$ for all eigenvalues σ at every swirl level ω. A similar conclusion is drawn from the flow simulations of Rusak *et al.* (1998*a*). Although not needed for the following analysis, it is strongly expected that $\sigma_I = 0$ and $\epsilon_I = 0$ also in our case.

We study now the equations resulting from the real parts of (43)–(44). Note that according to the result of the previous paragraph, terms of the order $\sigma_I \epsilon_I$ are much smaller than terms of the order σ_R and $\Delta\Omega$ and may be neglected. Using (60) in (43) and (44) gives (as shown in Appendix D),

$$
\epsilon_R[\mathscr{L}(\phi_R(x, y); \Omega_1) - \mathscr{L}(\phi_R(0, y); \Omega_1)] - \sigma_R \int_0^x \mathscr{L}_1(\psi_{1c}(x', y), \rho_{1c}(x', y); \Omega_1) \, \mathrm{d}x'
$$

$$
+ \Delta\Omega \, \mathscr{L}_3(\psi_{1c}(x, y), \rho_{1c}(x, y); \Omega_1) = 0. \tag{63}
$$

The functional $\mathscr{L}(\phi_R(x, y); \Omega_1)$ in (63) is the same as defined in (51). In the functional $\mathscr{L}(\phi_R(0, y); \Omega_1)$, the condition $\phi_{Rxx}(0, y) = 0$ is used. The functionals $\mathscr{L}_1$ and $\mathscr{L}_3$ in (63) are given by

$$
\mathscr{L}_1(\psi_{1c}(x, y), \rho_{1c}(x, y); \Omega_1)
$$

$$
= -\frac{T_0 - M_0^2 w_0^2}{T_0} \left\{ \frac{2}{w_0} \left(\frac{\psi_{1cxx}}{2y} + \psi_{1cyy} \right) - \frac{w_{0yy}}{w_0^2} \psi_{1c} \right.
$$

$$
\left. + \gamma M_0^2 \left[\left(\frac{\Omega_1 K_0^2}{4y^2 w_0^2} - \frac{4w_{0y}}{w_0} \right) \rho_{1c} - 3\rho_{1cy} \right] \right\}
$$

$$
- \gamma M_0^2 \left\{ \frac{\Omega_1 K_0^2}{4y^2 w_0 T_0} \left[2M_0^2 w_0 S(y) + \frac{T_0 - 3M_0^2 w_0^2}{w_0} \rho_{1c} \right. \right.
$$

$$
\left. + \frac{w_{0y}}{\gamma w_0}(\Phi(y) - \psi_{1c}) - \frac{2}{\gamma}(\Phi_y(y) - \psi_{1cy}) \right]
$$

$$
- \frac{T_0 - M_0^2 w_0^2}{w_0 T_0} \left[\frac{w_0^2}{T_0 - M_0^2 w_0^2} \left(2M_0^2 w_0 S(y) + \frac{T_0 - 3M_0^2 w_0^2}{w_0} \rho_{1c} \right. \right.
$$

$$
\left. \left. \left. + \frac{w_{0y}}{\gamma w_0}(\Phi(y) - \psi_{1c}) - \frac{2}{\gamma}(\Phi_y(y) - \psi_{1cy}) \right) \right]_y \right\}, \tag{64}
$$

$$\mathscr{L}_3(\psi_{1c}(x, y), \rho_{1c}(x, y); \Omega_1) = \frac{T_0 - M_0^2 w_0^2}{T_0} \frac{K_0 K_{0y}}{2y^2 w_0^2} \psi_{1c} + \gamma M_0^2 \frac{T_0 - M_0^2 w_0^2}{T_0} \left\{ \frac{K_0^2}{4y^2 w_0} \rho_{1c} \right.$$

$$+ \frac{(\gamma - 1)}{\gamma} \frac{K_0^2}{4y^2 w_0 (T_0 - M_0^2 w_0^2)} \left(\frac{\Omega_1 K_0^2}{4y^2 w_0} - 2w_{0y} \right) \psi_{1c}$$

$$\left. - \frac{(\gamma - 1)}{\gamma} w_0 \left[\frac{K_0^2}{4y^2 w_0 (T_0 - M_0^2 w_0^2)} \psi_{1c} \right]_y \right\}. \tag{65}$$

Multiplication of (63) by the adjoint function $\psi_{1c}^*(x, y)$ and the integration over the flow domain $0 \leqslant x \leqslant x_0$ and $0 \leqslant y \leqslant 1/2$ results in

$$\epsilon_R \int_0^{x_0} \int_0^{1/2} [\mathscr{L}(\phi_R(x, y); \Omega_1) - \mathscr{L}(\phi_R(0, y); \Omega_1)] \psi_{1c}^*(x, y) \, \mathrm{d}y \, \mathrm{d}x$$

$$- \sigma_R \int_0^{x_0} \int_0^{1/2} \left[\int_0^x \mathscr{L}_1(\psi_{1c}(x', y), \rho_{1c}(x', y); \Omega_1) \, \mathrm{d}x' \right] \psi_{1c}^*(x, y) \, \mathrm{d}y \, \mathrm{d}x$$

$$+ \Delta\Omega \int_0^{x_0} \int_0^{1/2} [\mathscr{L}_3(\psi_{1c}(x, y), \rho_{1c}(x, y); \Omega_1)] \psi_{1c}^*(x, y) \, \mathrm{d}y \, \mathrm{d}x = 0. \tag{66}$$

Calculation shows that the first term in (66) vanishes. Therefore, we find from (66) that σ_R is given by

$$\frac{\sigma_R}{\Delta\Omega} = \frac{\displaystyle\int_0^{x_0} \int_0^{1/2} \mathscr{L}_3(\psi_{1c}(x, y), \rho_{1c}(x, y); \Omega_1) \psi_{1c}^*(x, y) \, \mathrm{d}y \, \mathrm{d}x}{\displaystyle\int_0^{x_0} \int_0^{1/2} \left[\int_0^x \mathscr{L}_1(\psi_{1c}(x', y), \rho_{1c}(x', y); \Omega_1) \, \mathrm{d}x' \right] \psi_{1c}^*(x, y) \, \mathrm{d}y \, \mathrm{d}x}. \tag{67}$$

This result shows a linear relationship between the real part of the growth rate of the perturbation and the change of swirl ratio around the critical level ω_1. It can be seen from (67) that as M_0 tends to zero and $T_0 = 1$, the stability relationship of Wang & Rusak (1996a) for incompressible vortex flows is recovered. Also, it can be shown for model vortices such as the solid-body rotation, the Rankine vortex, the Burgers vortex, or the Q-vortex and for all subsonic Mach numbers that the ratio on the right-hand side of (67) is positive. This result shows that $\sigma_R < 0$ when $\Delta\Omega < 0$ and for compressible supercritical swirling flows with $\omega < \omega_1$, the mode of disturbance is asymptotically stable. As $\Delta\Omega$ tends to 0 also σ_R tends to 0 and the mode of disturbance is neutrally stable when $\omega = \omega_1$ (the critical level). However, $\sigma_R > 0$ when $\Delta\Omega > 0$ and therefore compressible subcritical swirling flows with $\omega > \omega_1$ are unstable. This proves that the critical swirl ratio for a compressible vortex flow in a finite-length pipe is a point of exchange of stability for compressible columnar swirling flows.

To demonstrate the change of $\sigma_R/\Delta\Omega$ with M_0 we study the case where the inlet axial velocity and temperature profiles are uniform, $w_0 = T_0 = 1$, and the circumferential velocity is given by a solid-body rotation profile, $K_0 = 2y$. Then, (67) results in

$$\frac{\sigma_R}{\Delta\Omega} = \frac{\pi^2}{4x_0} \frac{\displaystyle\int_0^{1/2} \Phi^* I_3 \, \mathrm{d}y}{\displaystyle\int_0^{1/2} \Phi^* I_1 \, \mathrm{d}y} \tag{68}$$
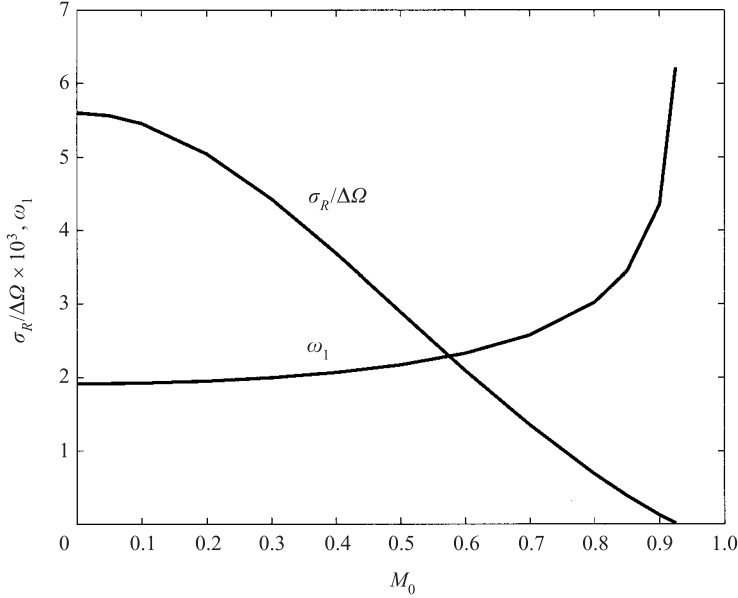
FIGURE 2. The growth-rate ratio $\sigma_R/\Delta\Omega$ and the critical swirl number ω_1 as function of Mach number for a solid-body rotation flow in a pipe with $x_0 = 60$.

where

$$I_1 = \left[\frac{\pi^2}{4x_0^2 y}M_0^2\left(M_0^2 - 2\right) + \frac{4}{y}\left(1 + M_0^2 - M_0^4\right)\Omega_1 + 2(\gamma - 1)M_0^4\Omega_1^2\right]\Phi$$
$$+ 2\gamma M_0^2\left(1 - M_0^2\right)\Omega_1\Phi_y,$$

$$I_3 = 2\left[\frac{(1 - M_0^2)}{y} + (\gamma - 1)M_0^2\Omega_1\right]\Phi - \gamma M_0^2\Phi_y.$$

We use results for ω_1 and $\Phi(y)$ in figures 1 and 2 in Rusak & Lee (2002) and results for $\Phi^*(y)$ in figure 1 to compute $\sigma_R/\Delta\Omega$ at various Mach numbers, see computed results in figure 2. It can be seen that the growth rate ratio $\sigma_R/\Delta\Omega$ is positive for all Mach numbers, but decreases as Mach number M_0 is increased. This ratio vanishes at the limit Mach number $M_{0\ limit} \sim 0.925$ at which the critical swirl ω_1 tends to infinity.

5. Conclusions

The linear stability of a compressible inviscid axisymmetric and rotating columnar flow of a prefect gas in a finite-length straight circular pipe can be investigated. This work extends the analysis of Wang & Rusak (1996a) to include the influence of Mach number on the flow dynamics. A well-posed model of the unsteady motion of a swirling flow, with inlet and outlet conditions that may reflect the physical situation, is formulated. The linearized equations of motion for the evolution of infinitesimal axially symmetric disturbances is derived. A general mode of disturbance, that is not limited to the axial-Fourier mode, is introduced and an eigenvalue problem is developed. It is found that a neutral mode of disturbance exists at 'the critical swirl ratio for a compressible vortex flow' defined by Rusak & Lee (2002). The flow changes its stability characteristics as the swirl ratio increases across this critical level. When

the swirl ratio is below the critical level (supercritical flow), an asymptotically stable mode is found and, when it is above the critical level (subcritical flow), an unstable mode of disturbance may develop. This result cannot be predicted by any of the previous stability criteria. When the characteristic Mach number of the base flow tends to zero, the results are the same as found for incompressible swirling flows in pipes. The growth rate ratio $\sigma_R / \Delta\Omega$ is positive for all Mach numbers, but decreases as Mach number M_0 is increased. This ratio vanishes at the limit Mach number at which the critical swirl ω_1 tends to infinity. These results match the conclusions from the simulations of Melville (1996) and Herrada *et al.* (2000).

The results of this paper show that the exchange of stability at swirl levels around the critical state found in incompressible vortex flows also dominates the dynamics of compressible swirling flows. The instability mechanism is again characterized by the travel of a certain mode of azimuthal vorticity disturbances as function of the swirl level ω of the incoming flow to the pipe. These disturbances can move upstream and their speed of motion grows with ω. When ω is less than ω_1 the azimuthal vorticity disturbances have a speed less than the axial speed of the incoming flow and, therefore, are washed out from the pipe and the base columnar flow is asymptotically stable. At $\omega = \omega_1$, there is a critical balance between the speed of the vorticity disturbances trying to move upstream and the axial flow entering the pipe and a neutrally stable mode of disturbance exists. When ω is greater than ω_1 the azimuthal vorticity disturbances are able to move upstream, but are blocked by the relatively fixed conditions of the axial and circumferential speeds at the pipe inlet, which are induced by the vortex generator ahead of the pipe. Therefore, these disturbances are trapped, accumulate, and initiate an instability process. The work of Wang & Rusak (1997a) showed that this instability mode is related to the vortex breakdown process in incompressible swirling flows. It is strongly expected that a similar situation occurs in compressible swirling flows.

The present paper and Rusak & Lee (2002) also show that, in subsonic vortex flows, the compressibility effects increase the critical swirl to higher values as well as reduce the absolute value of growth rate of the special mode of disturbances. The compressibility effects may be explained by the circumferential component of the vorticity transport equation for an unsteady axisymmetric compressible and inviscid flow (it can be derived in a similar way to that presented in Rusak & Lee (2002, pp. 316–317):

$$\left(\frac{-\bar{\chi}}{\bar{\rho}}\right)_{\bar{t}} + \bar{w}\left(\frac{-\bar{\chi}}{\bar{\rho}}\right)_{\bar{x}} + \bar{u}\left(\frac{-\bar{\chi}}{\bar{\rho}}\right)_{\bar{r}}$$
$$= \frac{2\bar{K}\bar{K}_{\bar{r}}\bar{u}}{\bar{\rho}\bar{w}\bar{r}^4} + \frac{\bar{K}^2}{\bar{\rho}\bar{r}^4}\frac{\bar{T}_{\bar{x}}}{\bar{T}} + \frac{1}{\bar{\rho}\bar{T}\bar{r}}(\bar{T}_{\bar{r}}(\bar{w}_{\bar{t}} + \bar{u}\bar{w}_{\bar{r}} + \bar{w}\bar{w}_{\bar{x}}) - \bar{T}_{\bar{x}}(\bar{u}_{\bar{t}} + \bar{u}\bar{u}_{\bar{r}} + \bar{w}\bar{u}_{\bar{x}})), \quad (69)$$

where $\bar{\chi} = \bar{\eta}/\bar{r}$ and we denote as $\bar{\eta}$ the azimuthal component of the vorticity. Equation (69) shows that the change in time and the convection of the property $(-\bar{\chi}/\bar{\rho})$ is balanced by the stretching effect (first term on the right-hand side of (69)), baroclinic effects resulting from the interaction between the swirl, density and axial temperature gradient (the second term), and baroclinic effects resulting from the interaction between the radial and axial speeds, density and temperature gradients (the third term). When (14) is used and $T_0(r) = 1$ is used, it can be shown that the third term of the right-hand side of (69) is of higher order and may be neglected. Then, the first and second terms show that the change of density with the increase of Mach number may affect the motion of the azimuthal vorticity disturbance and the swirl level for

a critical balance. In the case of a flow perturbation with $\bar{u} > 0$, the present analysis shows that a related increase in temperature around the pipe centreline with $\bar{T}_{\bar{x}} > 0$ and in density $\bar{\rho}$. These changes increase with the flow Mach number and reduce the size of the stretching term in (69) as Mach number is increased. Therefore, the resistance to the motion of the azimuthal vorticity disturbance is reduced with the increase of Mach number and as a result the growth-rate ratio $\sigma_R / \Delta\Omega$ decreases with M_0 and a higher level of swirl is needed to create a critical balance. The results (67), (68) and figure 2 and the computed examples in Rusak & Lee (2002) demonstrate this fundamental nature of compressible vortex flows.

Equation (69) also shows that when the perturbations are sufficiently small, the x-derivative of temperature dominates the evolution of the azimuthal vorticity, whereas the r-derivative of temperature appears only in higher-order terms. Therefore, the present linear stability results are not limited to the isothermal constant inlet temperature profile that is used in the example shown above. These results also hold for realistic inlet temperature profiles such as monotonically increasing or decreasing with r that have small deviations from the isothermal state. However, it is expected that when the perturbations grow, the r-derivative of temperature in (69) also becomes important and affects the global dynamics of the flow and transition to breakdown. Then, the nature of the inlet temperature profile may be important and result in a complicated behaviour that should be further analysed by global analysis techniques and numerical simulations.

The present work together with Rusak & Lee (2002) also demonstrate that compressible vortex flows are relatively more stable than incompressible vortex flows at the same incoming flow swirl ratio, specifically for swirl levels where $\omega_{1M_0=0} \lesssim \omega < \omega_{1M_0>0}$. Therefore, we find that the axisymmetric breakdown of high-Reynolds-number compressible vortex flows may be delayed to higher swirl ratios with the increase of the incoming flow Mach number.

REFERENCES

ALTHAUS, W., BRUECKER, CH. & WEIMER, M. 1995 Breakdown of slender vortices. In *Fluid Vortices* (ed. S. I. Green), pp. 373–426. Kluwer.

ASH, R. L. & KHORRAMI, M. R. 1995 Vortex stability. In *Fluid Vortices* (ed. S. I. Green), pp. 317–372. Kluwer.

BENJAMIN, T. B. 1962 Theory of the vortex breakdown phenomenon. *J. Fluid Mech.* **14**, 593–629.

BERAN, P. S. 1994 The time-asymptotic behaviour of vortex breakdown in tubes. *Computers Fluids* **23**, 913–937.

BRUECKER, CH. & ALTHAUS, W. 1995 Study of vortex breakdown by particle tracking velocimetry (PTV), Part 3: time-dependent structure and development of breakdown modes. *Exps. Fluids* **18**, 174–186.

DELERY, J. M. 1994 Aspects of vortex breakdown. *Prog. Aerospace Sci.* **30**, 1–59.

ESCUDIER, M. 1988 Vortex breakdown: observations and explanations. *Prog. Aerospace Sci.* **25**, 189–229.

GALLAIRE, F. & CHOMAZ, J.-M. 2001 Optimal control of vortex breakdown. *Bull. Am. Phys. Soc.* **46**, 158–159.

HERRADA, M. A., PREZ-SABORID, M. & BARRERO, A. 2000 Effects of compressibility on vortex breakdown. *Bull. Am. Phys. Soc.* **45**, 122.

HOWARD, L. N. & GUPTA, A. S. 1962 On the hydrodynamic and hydromagnetic stability of swirling flows. *J. Fluid Mech.* **14**, 463–476.

LEIBOVICH, S. 1984 Vortex stability and breakdown: survey and extension. *AIAA J.* **22**, 1192–1206.

LEIBOVICH, S. & STEWARTSON, K. 1983 A sufficient condition for the instability of columnar vortices. *J. Fluid Mech.* **126**, 335–356.

LESSEN, M., SINGH, P. J. & PAILLET, F. 1974 The stability of a trailing line vortex. Part 1. Inviscid theory. *J. Fluid Mech.* **63**, 753–763.

LOPEZ, J. M. 1994 On the bifurcation structure of axisymmetric vortex breakdown in a constricted pipe. *Phys. Fluids* **6**, 3683–3693.

LUDWIEG, H. 1960 Stabilitat der stromung in einem zylindrischen ringraum. *Z. Flugwiss.* **8**, 135–140.

MALKIEL, E., COHEN, J., RUSAK, Z. & WANG, S. 1996 Axisymmetric vortex breakdown in a pipe theoretical and experimental studies. *Proc. 36th Israel Annual Conf. on Aerospace Sciences*, 24–34 February.

MATTNER, T. W., JOUBERT, P. N. & CHONG, M. S. 2002 Vortical flow. Part 1. Flow through a constant-diameter pipe. *J. Fluid Mech.* **463**, 259–291.

MELVILLE, R. 1996 The role of compressibility in free vortex Breakdown. *AIAA Paper* 96-2075, June.

RAYLEIGH, LORD 1916 On the dynamics of revolving fluids. *Proc. R. Soc. Lond.* A**93**, 148–154.

RUSAK, Z. 1998 The interaction of near-critical swirling flows in a pipe with inlet vorticity perturbations. *Phys. Fluids* **10**, 1672–1684.

RUSAK, Z. 2000 Review of recent studies on the axisymmetric vortex breakdown phenomenon. *AIAA Paper* 2000–2529.

RUSAK, Z. & JUDD, K. P. 2001 The stability of non-columnar swirling flows in diverging streamtubes. *Phys. Fluids* **13**, 2835–2844.

RUSAK, Z., JUDD, K. P. & WANG, S. 1997 The effect of small pipe divergence on near-critical swirling flows. *Phys. Fluids* **9**, 2273–2285.

RUSAK, Z. & LEE, J. H. 2002 The effect of compressibility on the critical swirl of vortex flows in a pipe. *J. Fluid Mech.* **461**, 301–319.

RUSAK, Z., WANG, S. & WHITING, C. H. 1998*a* The evolution of a perturbed vortex in a pipe to axisymmetric vortex breakdown. *J. Fluid Mech.* **366**, 211–237.

RUSAK, Z., WHITING, C. H. & WANG, S. 1998*b* Axisymmetric breakdown of a Q-vortex in a pipe. *AIAA J.* **36**, 659–667.

SNYDER, D. O. & SPALL, R. E. 2000 Numerical simulation of bubble-type vortex breakdown within a tube-and-vane apparatus. *Phys. Fluids* **12**, 603–608.

SYNGE, L. 1933 The stability of heterogeneous liquids. *Trans. R. Soc. Canada* **27**, 1–18.

THOMPSON, K. 1987 Time dependent boundary conditions for hyperbolic systems. *J. Comput. Phys.* **68**, 1–24.

THOMPSON, P. A. 1988 *Compressible Fluid Dynamics*. Advanced Engineering Series.

TROMP, J. C. & BERAN, P. S. 1996 Temporal evolution of three-dimential vortex breakdown from steady, axisymmetric solutions. *AIAA J.* **34**, 632–634.

TROMP, J. C. & BERAN, P. S. 1997 The role of nonunique axisymmetric solutions in 3-D vortex breakdown. *Phys. Fluids* **9**, 992–1002.

WANG, S. & RUSAK, Z. 1996*a* On the stability of an axisymmetric rotating flow. *Phys. Fluids* **8**, 1007–1016.

WANG, S. & RUSAK, Z. 1996*b* On the stability of non-columnar swirling flows. *Phys. Fluids* **8**, 1017–1023.

WANG, S. & RUSAK, Z. 1997*a* The dynamics of a swirling flow in a pipe and transition to axisymmetric vortex breakdown. *J. Fluid Mech.* **340**, 177–223.

WANG, S. & RUSAK, Z. 1997*b* The effect of slight viscosity on near critical swirling flows. *Phys. Fluids* **9**, 1914–1927.